PHYSICAL REVIEW A **79**, 041602(R) (2009)

Dipole oscillations of confined lattice bosons in one dimension

Simone Montangero,[1,2] Rosario Fazio,[1,3] Peter Zoller,[4,5] and Guido Pupillo[4,5]
[1]*NEST-CNR-INFM and Scuola Normale Superiore, I-56156 Pisa, Italy*
[2]*Institut für Quanteninformationsverarbeitung, Universität Ulm, D-89069 Ulm, Germany*
[3]*International School for Advanced Studies (SISSA), I-34014 Trieste, Italy*
[4]*Institute for Theoretical Physics, University of Innsbruck, A-6020 Innsbruck, Austria*
[5]*Institute for Quantum Optics and Quantum Information, A-6020 Innsbruck, Austria*
(Received 10 October 2008; revised manuscript received 16 January 2009; published 7 April 2009)

We study the dynamics of a nonintegrable system comprising interacting cold bosons trapped in an optical lattice in one dimension by means of exact time-dependent numerical density-matrix renormalization group techniques. Particles are confined by a parabolic potential, and dipole oscillations are induced by displacing the trap center of a few lattice sites. Depending on the system parameters this motion can vary from undamped to overdamped. We study the dipole oscillations as a function of the lattice displacement, the particle density, and the strength of interparticle interactions. These results explain the recent experiment [C. D. Fertig *et al.*, Phys. Rev. Lett. **94**, 120403 (2005)].

DOI: 10.1103/PhysRevA.79.041602 PACS number(s): 67.85.−d, 03.75.Hh, 03.75.Lm, 05.30.Jp

Recent experiments with cold atoms [1–4] have provided realizations of nonequilibrium quantum many-body systems, allowing to address a number of fundamental questions. For example, the integrability of a many-body system has been demonstrated in Ref. [2] via the inhibition of thermalization in a one-dimensional (1D) Bose gas, which opened the way to theoretical studies of the relaxation dynamics of nonequilibrium many-body systems [5]. The dynamics of nonintegrable systems has been recently explored experimentally in Refs. [3,4] using interacting cold bosonic atoms trapped in an array of one-dimensional optical lattices and confined by a parabolic potential. Dipole oscillations were induced by displacing the center of the parabolic potential, and the dipole dynamics was studied by monitoring the position of the center of mass. A sudden transition from a regime of undamped motion to a regime of strongly damped motion was observed on increasing the lattice depth. Since damping of the center of mass oscillations is due to excitations in the optical lattice, the results obtained in [3,4] have provided precious diagnostic of the dynamical correlations of the many-body system, and thus have stimulated considerable theoretical interest [6–8].

Good agreement with the experimental results in [4] has been obtained in the regimes of very weak [7] and very strong interactions [8], where mean-field and extended fermionization techniques apply. However, it remains a fundamental challenge to understand the dipole dynamics in the regime of intermediate interactions, where the sudden localization transition occurs and the subtleties of 1D correlations do not allow (semi-)analytical treatments. With the aim to provide a comprehensive explanation of the experiment of Fertig *et al.* [4], in this Rapid Communication we study the dipole oscillations by means of a numerically exact time-dependent density-matrix-renormalization-group technique (tDMRG); see also [9]. We find very good agreement with the experimental results in the interesting regime of intermediate interactions. These results demonstrate that time-dependent numerical simulations with tDMRG have reached the same accuracy of current experiments with cold gases in the strongly correlated regime and thus represent a unique theoretical tool for quantitative comparisons and predictions for experiments in the cold atom context.

The experiment in [4] was performed in a parameter regime where the use of the following Bose-Hubbard Hamiltonian is microscopically justified [10];

$$H = -J\sum_j (b_j^\dagger b_{j+1} + \text{H.c.}) + \Omega\sum_j [j+\delta(t)]^2 n_j + \frac{U}{2}\sum_j n_j(n_j-1). \quad (1)$$

The first term on the r.h.s. of Eq. (1) describes the tunneling of bosons between neighboring sites with rate J (j labels the sites on the lattice). The second term is the parabolic potential with curvature Ω, $\delta(t)$ is a sudden displacement of the trap center, $\delta_0(t)=\delta\Theta(t)$ [with $\Theta(t)$ the Heaviside function], and $n_j=b_j^\dagger b_j$ is the density operator with bosonic creation (annihilation) operators $b_j^\dagger$ (b_i). The last term is the onsite contact interaction with energy U [10] (we set $\hbar=1$).

The sudden displacement on the trap center causes dipole oscillations of the bosons which can be analyzed experimentally by monitoring the time evolution of the center of mass (COM) $x_{\text{com}}=\Sigma_j j\langle n_j\rangle/N$, with N as the number of particles. The experiment of Ref. [4] was performed on an array of one-dimensional optical lattices where the number of particles in each 1D lattice varied from $N\simeq 80$ to zero. Thus, in order to provide a comprehensive and quantitative comparison with the experimental data, here we analyze the dipole dynamics as a function of δ, U/J, and the number of bosons N. We find that overdamped motion can occur as a function of δ for arbitrarily small interactions (Fig. 2), while in general sizeable interactions tend to extend the parameter region where localization occurs [11]. For a given Ω/J damping is found to depend exponentially on U/J and to be favored for small N. Figure 3(a), where the damping rate is shown as a function of the interaction and the number of bosons and, most important, Fig. 3(b), where we compare our numerics with the experimental data finding very good agreement in the intermediate range of interactions, allow for a different

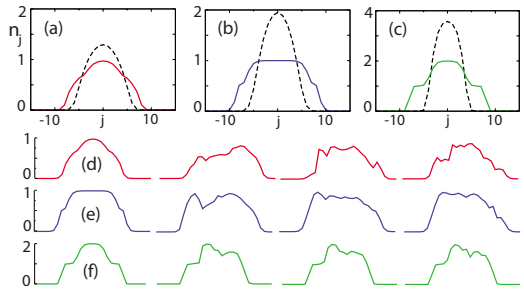

FIG. 1. (Color online) Relevant density distributions [panels (a)–(c)] (see text) and snapshots of the corresponding dipole dynamics [panels (d)–(f)]. (a) and (b) Density distribution for $N=11$ and 15 particles, respectively, for $\Omega/J=0.05623$. In each panel, the dashed and solid lines are $U/J=1$ and 20, respectively. The solid line in panel (b) corresponds to a Mott insulator. (c) Density distribution for $N=23$, $\Omega/J=0.4$, and $U/J=1$ and 20 (dashed and solid lines, respectively). The solid line corresponds to a cakelike structure. (d)–(f) Snapshots of the density distribution for cases (a)–(c), with $U/J=20$ and $\delta=4$, at times $tJ=0$, 30, 40, and 50. The dynamics of a few atoms in the Mott and cakelike configurations is frozen; however, residual oscillations can persist in the latter; see text.

explanation of the experiment of Ref. [4], based on the role of lattices with different N.

Three regimes are of interest for the dipole dynamics [see Fig. 1]: (a) for $4J \gtrsim \Omega(N/2)^2$ the density distribution is Gaussian or Thomas-Fermi type for $4J \gg U$ and $4J \simeq U$, respectively, and for $U \gg 4J$ onsite densities are smaller than one; (b) for $U > \Omega(N/2)^2 > 4J$ a Mott insulator with one particle per site is formed at the trap center; and (c) for $\Omega(N/2)^2 > U > 4J$ a shell structure is formed with a density $1 < n_j \leq 2$ at the trap center, surrounded by a Mott insulator with one particle per site. All the situations above occur in the experiment since N varies from one lattice to another. Therefore, in the following we are first interested in the dynamics of model systems as those in Fig. 1, which exemplify all three cases (a)–(c) above while still allowing for an extensive analysis in terms of all parameters N, Ω/J, and U/J, and then we address the experiment of Ref. [4] in the most interesting regime $U/J \gtrsim 4$.

The results presented below have been obtained by means of a tDMRG algorithm with a second-order Trotter expansion of H and time steps $0.01/J$ [12]. We take advantage of the conserved total number of particles N projecting on the corresponding subspace; the truncated Hilbert space dimension is up to $m=100$, while the allowed number of particles per site is $D=5$. All results below are found to be independent of this choice.

We first focus on the dipole dynamics as a function of the trap displacement δ in the regime of weak interactions. In this regime, mean-field theory predicts a sudden transition between undamped and overdamped motions via a dynamical instability at a critical displacement $\delta_c \simeq \sqrt{2J/\Omega}$ [11]. This value for δ_c can be understood by employing the exact solution of Eq. (1) in the noninteracting limit [13]. For energies $E \lesssim 4J$ the single-particle eigenstates of $H(t=0)$ are harmonic-oscillator-like modes extended around the center of the parabolic trap. However, for $E > 4J$ particles are Bragg scattered by the lattice and perform Bloch-type oscillations centered far from the trap center [14]. The particle localization corresponds to the population of these latter high-energy modes, which becomes significant for displacements $\delta \gtrsim \delta_c$ [13]. Our numerical results in the limit of weak interactions are shown in Figs. 2(a)–2(c), where dipole oscillations of the center of mass x_{com} are shown as a function of time t for different values of the displacement δ. In the simulations, as initial condition we use the ground-state wave function of the undisplaced potential, shifted by δ lattice sites. Upon increasing δ, the dynamics changes from undamped to damped, and the particles oscillate around the trap center. Upon increasing further the displacement [$\delta \gtrsim 5$ in panels (a) and (b)] the oscillations are overdamped and the COM slowly drifts toward the trap center or clings to the borders of the trap [case with $N=23$ of panel (c)]. This behavior corresponds to the localization transition predicted by mean-field theory. However, Fig. 2 shows that quantum fluctuations, properly accounted for by the tDMRG, smear out the transition into a smooth crossover between the undamped and the overdamped regimes.

Having established a connection with known results in the mean-field regime, we now present exact results for the particle localization in the interesting case of stronger interactions $U/J \gtrsim 1$ and $\delta \lesssim \delta_c$. We first focus on model systems and fix $\delta_c=6$ and the displacement $\delta=1<\delta_c$ such that for small interactions $U/J \lesssim 1$ the dynamical instability discussed above does not occur; e.g., for $U/J=1$ the dipole oscillations are undamped for all N [see Figs. 2(a) and 2(b)]. The dipole dynamics is then studied as a function of the ratio U/J. In particular, Fig. 3(a) shows the damping rate Γ of the dipole oscillations as a function of U/J for $N=11$, 15, and 28 [exemplifying cases (a), (b), and (c) above]. Here, Γ is calculated using the expression for underdamped oscillations $x_{\mathrm{com}}(t)=e^{-\Gamma t}[1-\cos(\Omega t+\phi_0)]+y_0$, with Γ, ϕ_0, and y_0 as fitting parameters. Two key observations are in order. (i) The damping rate depends *exponentially* on U/J for intermediate interaction strengths $2 \lesssim U/J \lesssim 6$ as $\Gamma/J \propto \exp[-\alpha(J/U)^{\beta}]$, with α and β as constants, a result which is not captured by mean field. For large N and small ratios $U \lesssim 0.1JN$ (e.g., $N=28$ and $U/J \lesssim 3$ in the figure) the numerical results are consistent with the phase-slip (instanton) prediction $\beta=0.5$ (dashed line) [15]. However, for larger interactions

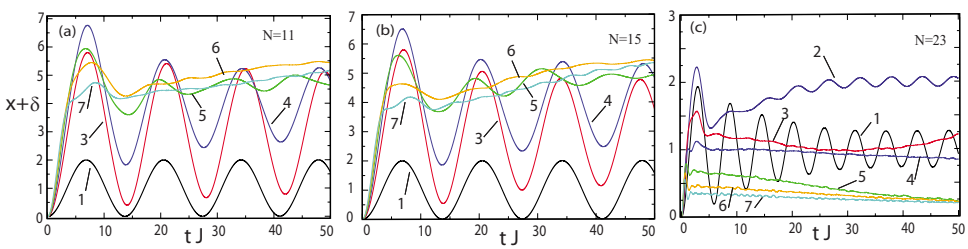

FIG. 2. (Color online) Center of mass position as a function of time for the cases of Figs. 1(a)–1(c) and $U/J=1$. The displacements δ are indicated in the figure. The critical displacement δ_c equals $\delta_c=6$ and 2 in panels (a)–(c), respectively.

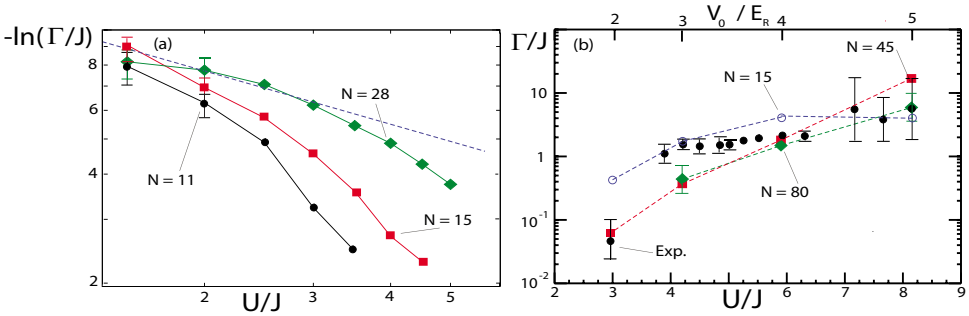

FIG. 3. (Color online) (a) Numerical results for the damping rate Γ of the dipole oscillations vs U/J for a fixed displacement $\delta=1<\delta_c$, with $\delta_c=6$ ($\Omega/J=0.05623$) and $N=11,15$, and 28 [cases (a)–(c) in the text]. The dashed line indicates the phase-slip (instanton) result $\Gamma/J\propto\exp(-\alpha\sqrt{J/U})$, with α as a constant (see text). (b) Damping rate Γ for the experiment of Ref. [4] vs U/J and the lattice depth V_0/E_R. The experimental data and the numerical results for $N=15,45,80$ are the black dots, the blue circles, the red squares, and the green diamonds, respectively.

we observe a much stronger decay, with β increasing up to the value $\beta\approx 2.2$ for $U\gtrsim 0.25JN$. Thus, for a given U/J the damping Γ is actually larger for *smaller* N, such that, e.g., for $N=11$ the dynamics is overdamped already for $U/J<4$. (ii) Eventually for large-enough interactions the oscillations are overdamped for all N. We find that for the cases $N=15$ and 28, this overdamping corresponds to the *formation of a Mott state* and a *cake structure* as in Figs. 1(b) and 1(c), respectively. In particular, for $N=15$ the particle localization occurs for $U/J\approx 4$, a value remarkably close to the superfluid/Mott-insulator quantum phase transition in a homogeneous lattice at commensurate filling and zero current. Once the Mott insulator is formed, no oscillations are further observed, as expected (see below). Thus, the results for $\delta<\delta_c$ naturally interpolate between the finite-current dynamical instability and the zero-current quantum phase transition [11]. In the following we show that points (i) and (ii) above have crucial consequences for the interpretation of the results of Ref. [4] in the most interesting regime of interactions $U/J\sim 4$.

In the experiment of Ref. [4], the decay of dipole oscillations was studied as a function of the optical lattice depth V_0 for a fixed displacement $\delta=8$, finding damping already for weak lattices $V_0/E_R>0.5$, with E_R as the recoil energy. The experimental data are shown as black dots in Fig. 3(b) as a function of V_0 in the range $2\lesssim V_0/E_R\lesssim 5$, where the use of Eq. (1) is justified [10,13], corresponding to the interesting regime of interactions $3\lesssim U/J\lesssim 8$. For $V_0/E_R<3$ and $V_0/E_R\gtrsim 3$ the value of the damping rate Γ has been extracted using formulas appropriate for underdamped and overdamped motion, respectively [4]. The most interesting experimental finding shown in Fig. 3(b) is the measurement of an abrupt transition from a weakly damped regime to an overdamped regime for a lattice depth $V_0/E_R\simeq 3$, where the damping rate Γ of the dipole oscillations increases by more than an order of magnitude. The physical mechanism behind this apparent transition has proven elusive.

In Fig. 3(b) the experimental results are compared to our numerical results for $N=80$, 45, and 15; green diamonds, red squares, and blue circles, respectively. The value $N=80$ has been chosen since it corresponds to the number of particles in the central 1D lattice of the array in the experiment, which is the most largely populated with $\langle n_j\rangle>1$ for all U/J, as in Fig. 1(c). Conversely, cases $N=15$ and 45 exemplify cases (a) and (b), with $\langle n_j\rangle<1$ and $\langle n_j\rangle=1$ for $U/J\gtrsim 4$, respectively. The figure shows a very good agreement between the numerical and the experimental results in the entire region $2\lesssim V_0/E_R\lesssim 5$ ($3\lesssim U/J\lesssim 8$). The low-density case $N=15$ shows the strongest damping for all values $2\lesssim V_0/E_R<5$. Cases $N=45$ and 80 underestimate Γ around the transition point $V_0/E_R\simeq 3$, while the agreement at $V_0/E_R\simeq 4$ is almost perfect. For $V_0/E_R\gtrsim 5$ all numerical results fall inside the experimental error bars; however, the case $N=45$ shows a stronger damping. The explanation of the results above stems from the observation that in the experiment δ_c varies between $\delta_c\sim 18$ and 15 for $3\lesssim V_0/E_R\lesssim 5$, and thus $\delta<\delta_c$ for all lattice depths. We can then use the results for the model systems of Fig. 3(a) to explain the experimental findings. That is, (i) the transition observed experimentally at $V_0/E_R\simeq 3$ is actually a *crossover*, where the 1D systems with the lowest number of particles tend to localize first, in agreement with the discussion of Fig. 3(a). Since in the experiment about 80% of the atoms are located in tubes with $\langle n_j\rangle\lesssim 1$, the observed strong damping at $V_0/E_R\simeq 3$ is a result of averaging over those tubes. (ii) For $V_0/E_R\gtrsim 5$, the dynamics of particles in the 1D systems with $\langle n_j\rangle=1$ ($N=45$ in the simulations) is completely frozen, due to the formation of a Mott insulator, and the overall mobility of the cloud is due to residual oscillations in lattices with lower ($N=15$) and higher ($N=80$) onsite densities. These oscillations have a different origin, as explained below. We notice that for $N=80$ numerical simulations have been also performed in [9], and our results agree with those. However, in contrast to [9] we here perform a detailed analysis for various N, which is necessary to explain the experiment.

The different behaviors of Γ for $N=15$, 45, and 80 and $U/J>4$ can be modeled as follows. In the low-density cases with $N=15$ and 45 the tendency to localization is explained by noting that interactions broaden the spatial width of the atom cloud, until the onsite density falls below one [see also Figs. 1(a) and 1(b)]. In this case, the low-energy physics maps into that of an extended cloud of noninteracting fermions, with single-band Hamiltonian [13],

$$\tilde{H}_1(t)=-J\sum_{\langle i,j\rangle}c_i^\dagger c_j+\Omega\sum_j[j-\delta(t)]^2c_j^\dagger c_j,$$

with c_j and $c_j^\dagger$ as fermionic operators. For large-enough displacements δ, the fermions largely occupy localized modes

of the single-particle spectrum discussed above, and the COM motion is overdamped. In particular, for $N=45$ [case (b)] the COM motion is frozen due to the formation of a (band) insulator at time $t=0$, while for $N=15$ the COM remains more mobile. This is explained by noting that in the latter case the population of localized modes is reduced since $w+\delta$ is barely on the order of δ_c, with w as the computed half-width of the atom cloud (e.g., $w\approx 11$ for $V_0/E_R=5$). The dynamics of interacting particles at large density, e.g., $N=80$ in Fig. 3(b), can be modeled starting from the case of largest interactions $U/J\gg 1$, where the density profile has a cakelike structure [Fig. 1(c)]. This situation is well described by an extended fermionization model [8,16,17], where Eq. (1) is replaced by an effective Hamiltonian with two coupled Fermi bands separated by an energy U [17],

$$\tilde{H}_2(t) = -J\sum_{\langle i,j\rangle}[c_i^\dagger c_j + 2d_i^\dagger d_j + \sqrt{2}(c_i^\dagger d_j + d_i^\dagger c_j)] + \sum_j (\Omega[j+\delta(t)]^2 c_j^\dagger c_j + \{\Omega[j+\delta(t)]^2 + U\} d_j^\dagger d_j), \tag{2}$$

with the operators c_j and $c_j^\dagger$, and d_j and $d_j^\dagger$ referring to the lower and higher-energy bands of width $4J$ and $8J$, respectively. Oscillations in this limit are due to the dynamics of the (delocalized) d_j fermions of Eq. (2) in the higher-energy band, while c_j fermions are frozen in a (band) insulator. Thus these residual oscillations have a different origin with respect to those described above for $N=15$. Their observation corresponds to probing the superfluidity of bosons with two particles per site in a homogeneous lattice in a local-density-approximation sense [18]. This picture, valid for $U/J\gg 1$ [8,17], can be extended to gain a qualitative insight in the dependence of the dipole oscillations on interactions for $4\lesssim U/J\lesssim 10$. In fact, neglecting the parabolic potential, in this regime the model of Eq. (2) suggests that the spectrum is continuum since the gap U between the two Fermi bands is smaller than their total width. It is thus plausible that Bloch-type oscillations of the particles are here suppressed and that transport is restored. However, for $U\gtrsim 5J$ the energy spectrum develops a gap again around $4J$, and thus transport in the lower-energy band is inhibited. Residual current is then due to delocalized particles in the higher-energy band, as explained above. We notice that this picture is consistent with our numerical findings for $U/J>5$ in Fig. 3(b).

In conclusion, we have explained the experiment in [4] in the most interesting regime of intermediate interactions. The very good agreement between experimental and tDMRG results demonstrates the latter as a unique tool for quantitative comparisons with cold gas experiments in the strongly correlated regime in one dimension.

Discussions with A. M. Rey, C. J. Williams, and C. W. Clark are gratefully acknowledged. This work was supported by OLAQUI, NAMEQUAM, FWF, MURI, EUROSQIP, SFB/TRR21, and DARPA and developed using the DMRG code released within the PwP project (www.dmrg.it).

[1] L. Pezzè *et al.*, Phys. Rev. Lett. **93**, 120401 (2004); N. Strohmaier *et al.*, *ibid.* **99**, 220601 (2007); J. Mun *et al.*, *ibid.* **99**, 150604 (2007); L. E. Sadler *et al.*, Nature (London) **443**, 312 (2006).

[2] T. Kinoshita, T. Wenger, and D. S. Weiss, Nature (London) **440**, 900 (2006).

[3] T. Stoferle, H. Moritz, C. Schori, M. Kohl, and T. Esslinger, Phys. Rev. Lett. **92**, 130403 (2004).

[4] C. D. Fertig *et al.*, Phys. Rev. Lett. **94**, 120403 (2005).

[5] M. Rigol, V. Dunjko, V. Yurovsky, and M. Olshanii, Nature (London) **452**, 854 (2008); Phys. Rev. Lett. **98**, 050405 (2007); C. Kollath, A. M. Lauchli, and E. Altman, *ibid.* **98**, 180601 (2007); S. R. Manmana, S. Wessel, R. M. Noack, and A. Muramatsu, *ibid.* **98**, 210405 (2007).

[6] A. Polkovnikov and D.-W. Wang, Phys. Rev. Lett. **93**, 070401 (2004); M. Rigol, V. Rousseau, R. T. Scalettar, and R. R. P. Singh, *ibid.* **95**, 110402 (2005); J. Gea-Banacloche, A. M. Rey, G. Pupillo, C. J. Williams, and C. W. Clark, Phys. Rev. A **73**, 013605 (2006); A. V. Ponomarev and A. R. Kolovsky, Laser Phys. **16**, 367 (2006); M. Snoek and W. Hofstetter, Phys. Rev. A **76**, 051603(R) (2007).

[7] J. Ruostekoski and L. Isella, Phys. Rev. Lett. **95**, 110403 (2005).

[8] G. Pupillo *et al.*, N. J. Phys. **8**, 161 (2006).

[9] I. Danshita and C. W. Clark, Phys. Rev. Lett. **102**, 030407 (2009).

[10] D. Jaksch, C. Bruder, J. I. Cirac, C. W. Gardiner, and P. Zoller, Phys. Rev. Lett. **81**, 3108 (1998).

[11] A. Smerzi, A. Trombettoni, P. G. Kevrekidis, and A. R. Bishop, Phys. Rev. Lett. **89**, 170402 (2002); E. Altman, A. Polkovnikov, E. Demler, B. I. Halperin, and M. D. Lukin, *ibid.* **95**, 020402 (2005).

[12] A. J. Daley *et al.*, J. Stat. Mech.: Theor. Exp. (2004), P04005; S. R. White and A. E. Feiguin, Phys. Rev. Lett. **93**, 076401 (2004); U. Schollwöck, Rev. Mod. Phys. **77**, 259 (2005); G. De Chiara *et al.*, J. Comput. Theor. Nanosci. **5**, 1277 (2008).

[13] A. M. Rey, G. Pupillo, C. W. Clark, and C. J. Williams, Phys. Rev. A **72**, 033616 (2005).

[14] M. Rigol and A. Muramatsu, Phys. Rev. A **70**, 031603(R) (2004); C. Hooley and J. Quintanilla, Phys. Rev. Lett. **93**, 080404 (2004).

[15] A. Polkovnikov, E. Altman, E. Demler, B. Halperin, and M. D. Lukin, Phys. Rev. A **71**, 063613 (2005); D. McKay *et al.*, Nature (London) **453**, 76 (2008).

[16] G. Pupillo, C. J. Williams, and N. V. Prokof'ev, Phys. Rev. A **73**, 013408 (2006).

[17] M. Popp *et al.*, N. J. Phys. **8**, 164 (2006).

[18] M. P. A. Fisher, P. B. Weichman, G. Grinstein, and D. S. Fisher, Phys. Rev. B **40**, 546 (1989).